Solution-Processed Nanostructured CdS Thin Film with Improved Optoelectronic Properties

Ravi Mudike[a], Sanjay R. Dhage[*b], Prasanna D Shivaramu[a], Dinesh Rangappa[*a]

[a]*Department of Applied Sciences (Nanotechnology), Visvesvaraya Technological University, Centre for Postgraduate Studies, Muddenahalli, Chikkaballapur-562 101, India.*

[b] *International Advanced Research Centre for Powder Metallurgy and New Materials (ARCI), Hyderabad, India.*

* dhage@arci.res.in, dineshrangappa@gmail.com

Received: 11.3.23, Revised: 27.4.23 Accepted: 28.4.23

Abstract

Nanostructured CdS thin films are essential for efficient electron transport and they act as an ideal buffer layer in CIGS/CZTS/CdTe thin-film solar cells. Herein, low-temperature processed CdS nanostructured thin film on a glass substrate by chemical bath deposition for its application in optoelectronic devices is reported. As synthesized, CdS nanostructured thin films are exhibited polycrystalline, confirmed using X-ray diffraction/transmission electron microscopy. Further, polycrystalline (hexagon/cubic) nature reconfirmed by Raman band at 305 cm^{-1} of as-grown films. The surface morphology and EDS of CdS thin films reveal uniformity on the surface with non-cuboid nanoparticles and nearly stoichiometric. The optical band gap of CdS nanostructured thin films was found to be 2.3 eV, properties indicating its suitability as a buffer layer in CIGS/CZTS thin-film solar cells.

Keywords: CdS thin film, nanostructure, chemical bath deposition, Raman Spectra.

1. Introduction

Cadmium sulfide (CdS) is the most promising n-type semiconductor material in thin-film (CdTe/CIGS/CZTS) solar cells and next-generation optoelectronic devices; because of its direct bandgap (2.42 eV)[1], high absorption coefficient[2,3], having an absorption edge at 510 nm[4,5]. Researchers have reported the confirmable coating of CdS nanostructured film via a solution-based approach on CdTe/CIGS/CZTS layer to fabricate a solar cell device[6–9]. It is

inexpensive and forms a better interface with an absorber material layer. The better interface minimizes the recombination and leakage current at the junction[10,11]. The CdS nanostructured film as buffer layer used in solar cells have exhibited an efficiency of 23.35% for CIGS and 12.6% for CZTSSe[12,13].

CdS films are durable due to the lower lattice miss matching with the absorber layer and it offers faster electron transport at the interface. CdS layer can be deposited on the solar absorber layer using vacuum and non-vacuum techniques. Vacuum evaporation (VE)[14], chemical bath deposition (CBD)[15,16], spray pyrolysis (SP)[17], chemical vapor deposition[18], successive ionic layer adsorption and reaction[19] are some of the most effective methods for CdS thin film deposition. Among these, the CBD technique is more popular because of its cost-effective and low-temperature solution process. In addition, CdS films with high optical absorbance, low electrical resistivity, less recombination losses and better crystallinity can be obtained by this method which are very important for solar photovoltaic applications[20–22]. Electrical properties such as resistivity and the optical absorbance of CdS thin films strongly depend on the preparation and deposition conditions[23,24]. In this study, we have optimized the process conditions for the deposition of nanostructured CdS thin films to obtain high optoelectronic properties for its application in devices. The film's structural, electrical and optical properties were investigated and presented.

2. Experimental

2.1. Materials

Cadmium sulfate ($CdSO_4$, purity 99.99%), thiourea (CH_4N_2S, purity 99.0%) and ammonium hydroxide (25% NH_4OH) were purchased from Sigma-Aldrich and further used without purification.

CdS nanostructure film growth process and characterization

The CdS precursor solution was prepared by dissolving cadmium sulfate (0.16 M), thiourea (0.6 M) and ammonium hydroxide (7.5 ml) into DI-water at room temperature. Before the deposition of films, the soda-lime glass was cleaned following the standard procedure reported[25]. Subsequently, the as-prepared solution was used to grow CdS nanostructured films on a cleaned soda-lime glass substrate via chemical bath deposition process at 60 ^{0}C with various deposition times of 15 and 35 min and pH of the solution maintained at 10. For the 15 min deposition time of CdS thin-film and the 35 min deposition time CdS thin-film hereinafter called CdS-A and CdS-B, respectively. After the deposition reaction, the formed yellow precipitate (collected using the centrifugation process for analysis) and as grown

nanostructured films on soda-lime glass substrate were annealed at 300 ^{0}C for 2 h in the muffle furnace.

The morphology and elemental compositions of CdS powder and films were studied using scanning electron microscopy (Hitachi S-4300 SE/N, USA). The formation of the CdS phase was confirmed using the X-ray Diffraction (XRD) analysis (D8 Advance, Bruker) and the nanoparticle size was studied by Transmission Electron Microscopy (TEM) (FEI Tecnai G20 20 XTWIN). The film thickness was estimated using the X-ray Fluorescence Spectrometer (XRF). A Varian Cary 5E UV-Vis-NIR spectrophotometer was used to record the optical transmittance in the 250-2000 nm wavelength range.

3. Results and discussion

In photovoltaic devices, n-type semiconducting material plays a crucial role in transporting the charge carriers. It improves the open-circuit voltage of the device, here n-type CdS nanostructured films on a soda-lime glass substrate by a low-temperature solution process with variable time durations (15 and 35 min) and their digital photographs are shown in **Figure 1(a).** The crystallinity and phase of CdS nanostructured thin films and Nanoparticles' structural properties were investigated using TEM, XRD, and Raman spectroscopy. **Figure 1(b)** shows the XRD pattern of CdS nanostructured films on the glass substrate, it reveals the polycrystalline nature of CdS film. The peaks position at 25.1^0, 26.7^0, 28.2^0, 31.02^0, 44^0 and 52.03^0 indexed are corresponding to the (100), (111), (101), (200), (220) and (111) planes of cubic phase (JCPDS No.: 04-014-0285) and hexagonal phase (JCPDS No.: 01-074-9664), confirming the mixed-phase CdS film. Moreover, the diffraction peak corresponding to CdO can be seen in CdS-A and CdS-B samples. It is due to partial oxidation of cadmium and the evaporation of sulfur by annealing the films at 300 ^{0}C, supported by the earlier report [26]. However, the diffraction peaks corresponding to CdO have not appeared in the nanoparticle sample. The crystalline size was calculated using the Debye-Scherrer formula, and the average crystalline size of 8-12 nm was obtained. Interestingly, the CdS nanoparticle diffraction peaks have low-intensity broader peaks due to the apparent effect of crystalline size.

CdS nanostructured thin films were scratched and removed from the glass substrate and dispersed in the solvent to reconfirm the crystallinity and particle size by TEM **Figure 1(c)** shows the SAED pattern of CdS nanostructures indicating high crystallinity of the film. The SAED pattern reveals that the CdS nanostructure is polycrystalline and agrees with the XRD pattern. The reflected ring pattern was indexed and these rings correspond to the (111), (200),

(220) and (111) diffraction planes. Furthermore, CdS structural properties were also determined and reconfirmed using Raman spectroscopy. The Raman spectrum revealed two longitudinal optical (LO) phonon peaks at ~ 300 cm^{-1} and ~ 600 cm^{-1}, as shown in Fig. 1 (d). The hexagonal CdS Raman shift LO modes were observed at the same wavenumbers [18]. We observed that the 300 cm^{-1} peak is a significant phonon peak for all cases. FWHM reveals that CdS nanostructure films have higher crystallinity than CdS nanoparticles. However, the peak intensity is high and negligible spectral peak shift, reconfirming the identical quality of the film. It is worth mentioning here, the structural properties of the CdS nanostructured thin film grown on glass substrate are compared with the CdS nanoparticle, briefed in **Table 1**.

Figure 2. shows the surface morphology and elemental analysis of CdS nano-structured films at variable deposition times. The estimated particle size with a non-cuboid shape can be easily noticed from the surface morphology. **Figure 2(a),** the surface morphology of CdS-A nanostructured film deposited at 15 min reaction time, reveals a more agglomerate surface with an average particle size of 65 nm. Subsequently, elemental analysis was carried out at the particular area and the EDS spectra were inset of **Figure 2(a).** The EDS spectra provided the possible elemental composition with ratio, confirming the presence of Cd and S. Further increase in the reaction time from 15 to 35 min. The surface morphology/elemental composition of the CdS-B film is shown in **Figure 2(b),** indicating an increase in the particle size. In comparison, 35 min grown CdS nanostructured film has good adhesion, high particle size (an average particle size ~ 105 nm). However, it has more sulfur content (the EDS spectra inset **Figure 2(b)**) than the 15 min nanostructured film. TEM imaging was performed on the dispersed CdS nanoparticles to investigate the morphology, it reveals the particle size 10 nm and agrees with XRD data. CdS nanostructured thin film thickness was measured by X-Ray Fluorescence Spectrometer and found to be 125 nm and 194 nm for CdS-A and CdS-B thin films, respectively reiterate the increase in reaction time can lead to obtaining films with the higher thickness.

Figure 3.(a) shows the spectral transmittance curves of CdS-A & CdS-B nanostructured thin films recorded in UV-Vis-NIR spectrometer. The direct bandgap (E_g) of the films was determined by extrapolating the linear portion of the $(\alpha h\upsilon)^2$ versus $h\upsilon$ plot and taking the intercept on the X-axis, as shown in **Figure 3. (b).** The bandgap was calculated as 2.35 eV and 2.37 eV for CdS-A and CdS-B nanostructured thin films. Slight variation in bandgap

could be attributed to increasing deposition time, resulting in crystallinity improvement, in line with the earlier reported work[27].

4. Conclusion

The nanostructured CdS thin films via solution process were successfully prepared. The CdS nanoparticles are randomly oriented polytype structures or mixed type structures rather than hexagonal greenockite or cubic hawleyite structures. The hexagonal peaks are at 25.1^0 and 28.2^0 identified at the shoulder of the significant cubic (111) plane. Due to a longer reaction time, the grain size increased and nucleation enables lateral grain growth in the CdS-B film. The optical band gap energy of CdS film changes from 2.35 eV and 2.37 eV on increasing the deposition time from 15 to 35 min. The presented approach opens the possibility of growing crystalline CdS nanostructured architecture on the desired substrate at low temperatures for a range of optoelectronic applications such as solar cells.

Figures:

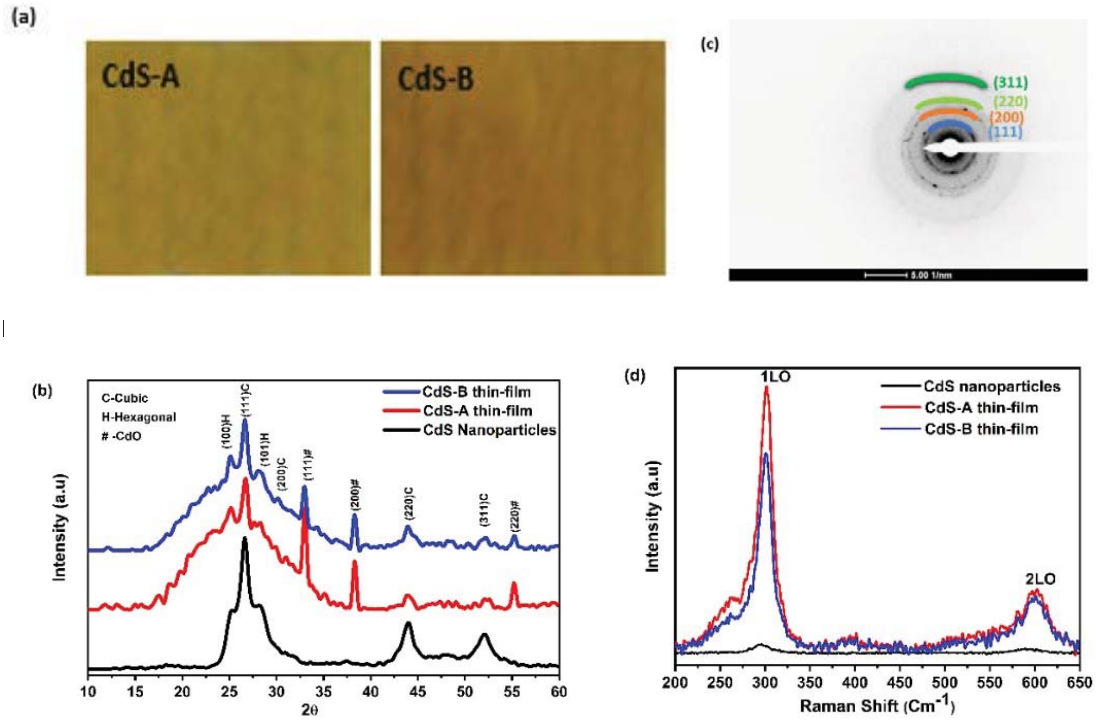

Figure 1. (a) Digital photographs, (b) XRD pattern, (c) TEM SAED pattern and (d) Raman spectra of CdS thin films deposited on glass at a variable time and of nanoparticles.

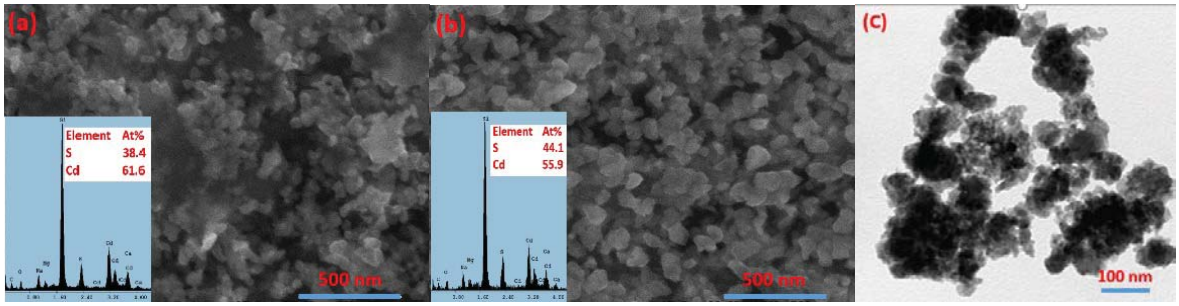

Figure 2. FESEM and EDS spectrum of CdS films deposited at (a) 15 min, (b) 35 min and (c) TEM morphology of CdS powder.

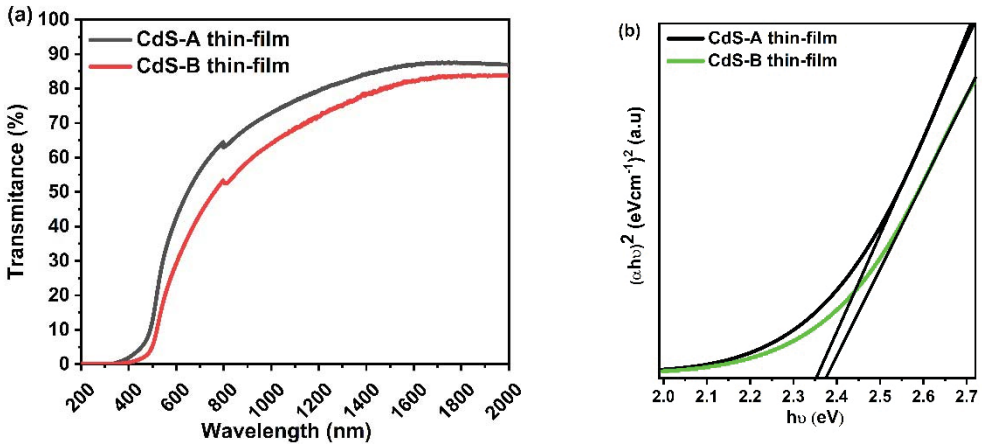

Figure 3. (a) Transmission spectra of CdS-A & CdS-B thin films and (b) $\alpha h\upsilon)^2$ versus $h\upsilon$ plot of CdS-A and CdS-B thin films.

Tables:

Table 1. Raman spectrum indexing of CdS NPs and CdS nanostructures films.

Sample Name	Raman shift (cm^{-1})	
	1LO	2LO
Standard CdS single crystal	306	604
CdS NPs	296	590
CdS-A nanostructured film	301	603
CdS-B nanostructured film	300	601

References

1 Y. Chen, W. Zhong, F. Chen, P. Wang, J. Fan and H. Yu, *J. Mater. Sci. Technol.*, **121**, 19, 2022.

2 M. Huang, C. Liu, P. Cui, T. Wu, X. Feng, H. Huang, J. Zhou and Y. Wang, *Environ. Sci. Technol.*, **55**, 13132.2021.

3 A. Hamid Rather, T. Umair Wani, R. Saleem Khan, A. Abdal-hay, S. Rather, J. Macossay and F. A. Sheikh, *Mater. Sci. Eng. B*, **286**, 116022, 2022.

4 Y. Lei, K. H. Ng, Y. Zhang, Z. Li, S. Xu, J. Huang and Y. Lai, *Chem. Eng. J.*, **434**, 134689,2022.

5 J. Yao, L. Wang, H. Zhou, Z. Xie, X. Zeng and C. Liu, *J. Colloid Interface Sci.*, **616**, 858, 2022.

6 R. Mudike, C. Sabbanahalli, J. B. Sriramoju, A. Bheemaraju, G. Halligudra, M. Muniyappa, M. P. Narayanaswamy, A. K. CS, P. D. Shivaramu and D. Rangappa, *Mater. Res. Bull.*, **146**, 111606, 2022

7 R. Mudike, A. Bheemaraju, T. Rasheed, N. Singh, S. R. Dhage, P. Doddakunche Shivaramu and D. Rangappa, *Ceram. Int.*, **48**, 35666, 2022.

8 G. K. U. P. Gajanayake, A. A. I. Lakmal, D. S. M. De Silva and B. S. Dassanayake, *J. Mater. Sci. Mater. Electron.*, **34**, 508, 2023.

9 O. Ahmad, I. Qasim, S. M. Hasnain, Z. ul Abdin, M. F. Nasir, M. I. Malik and A. Rashid, *Org. Electron.*, **117**, 106781, 2023.

10 H. Heriche, Z. Rouabah and N. Bouarissa, *Optik (Stuttg).*, **127**, 11751–11757, 2016.

11 M. T. Winkler, W. Wang, O. Gunawan, H. J. Hovel, T. K. Todorov and D. B. Mitzi, *Energy Environ. Sci.*, **7**, 1029, 2014.

12 M. Nakamura, K. Yamaguchi, Y. Kimoto, Y. Yasaki, T. Kato and H. Sugimoto, *IEEE J. Photovoltaics*, **9**, 1863, 2019.

13 W. Wang, M. T. Winkler, O. Gunawan, T. Gokmen, T. K. Todorov, Y. Zhu and D. B. Mitzi, *Adv. Energy Mater.*, **4**, 1, 2013.

14 S. Chander and M. S. Dhaka, *Thin Solid Films*, **638**, 179, 2017.

15 S. R. Dhage, H. A. Colorado and H. T. Hahn, *Mater. Res.*, **16**, 504. 2013.

16 P. Uday Bhaskar and S. R. Dhage, *Mater. Today Proc.*, **4**, 12525, 2017

17 M. Shkir, I. M. Ashraf, S. AlFaify, A. M. El-Toni, M. Ahmed and A. Khan, *Ceram. Int.*, **46**, 4652,2020

18 M. A. Buckingham, A. L. Catherall, M. S. Hill, A. L. Johnson and J. D. Parish, *Cryst.*

Growth Des., **17**, 907,2017.

19 C. E. Perez-Garcia, S. Meraz-Davila, G. Arreola-Jardon, F. De Moure-Flores, R. Ramírez-Bon and Y. V. Vorobiev, *Mater. Res. Express*, 7,015530,2020.

20 L. Guogen, C. Zimeng, B. R. B., P. Jingong, G. G. E. and C. K. K., *Conf. Rec. IEEE Photovolt. Spec. Conf.*, pp.003750,2011.

21 J. F. Akter, S. M. Zaman and R. M. Junaebur, *Mater. Renew. Sustain. Energy*, **8**, 1,2019

22 M. Abdulhur, K. Mankoshi, F. I. Mustafa, N. J. Hintaw, K. Kushiya, Y. Ohtake, P. U. Londhe and A. B. Rohom, in *Journal of Physics: Conf. Series*, pp. 1, 2018.

23 M. Maghouli and H. Eshghi, *Superlattices Microstruct.*, **128**, 327, 2019.

24 V. D. Moreno-Regino, F. M. Castañeda-de-la-Hoya, C. G. Torres-Castanedo, J. Márquez-Marín, R. Castanedo-Pérez, G. Torres-Delgado and O. Zelaya-Ángel, *Results Phys.*, **13**, 102238, 2019.

25 B. S. Yadav, A. C. Badgujar and S. R. Dhage, *Sol. Energy*, **157**, 507, 2017.

26 H. A. Colorado, S. R. Dhage and H. T. Hahn, *Mater. Sci. Eng. B Solid-State Mater. Adv. Technol.*, **176**, 116, 2011.

27 D. Petre, I. Pintilie, E. Pentia, I. Pintilie and T. Botila, *Mater. Sci. Eng. B Solid-State Mater. Adv. Technol.*, **58**, 238, 1999.